Applied Surface Science 665 (2024) 160309

Contents lists available at ScienceDirect

Applied Surface Science

journal homepage: www.elsevier.com/locate/apsusc

Short Communication

Real-time monitoring of Ti-Nb-Ta-Zr and commercially pure Ti interaction with H_2O_2 using atomic force microscopy and atomic emission spectroelectrochemistry

Agata Sotniczuk [a,b,*], Baojie Dou [c], Yangping Liu [d], Oumaïma Gharbi [e], Fan Sun [c], Halina Garbacz [b], Jeremy L. Gilbert [d], Kevin Ogle [c]

[a] NOMATEN Centre of Excellence, National Centre for Nuclear Research, A. Sołtana 7, 05-400 Otwock-Swierk, Poland
[b] Faculty of Materials Science and Engineering, Warsaw University of Technology, Woloska 141, 02-507 Warsaw, Poland
[c] Chimie-ParisTech, PSL University, Institut de Recherche ChimieParis, CNRS, F-75005 Paris, France
[d] The Clemson University-Medical University of South Carolina Bioengineering Program, 68 President Street, BE 325, Charleston, SC 29425, United States
[e] CNRS, Sorbonne Université, Laboratoire de Réactivité de Surface (LRS), 4 place Jussieu, F-75005 Paris, France

ARTICLE INFO

Keywords:
Titanium
AFM
AESEC
Biomaterials
Surface characterization

ABSTRACT

This study offers a new approach to analyze surface behavior of titanium biomaterials during their exposure to the H_2O_2-enriched fluid which simulates post-operative inflammatory conditions. In this work *in situ* AFM and AESEC tests were exploited to study the origin of initial inflammatory-induced degradation for commercially pure Ti (CP-Ti) and Ti-29Nb-13Ta-4.6Zr (TNTZ) alloy. Overall results indicate that initial interaction between H_2O_2 and TNTZ surface results only in dissolution of the alloy, while for CP-Ti both oxide formation and dissolution give important contribution to the degradation process. Proposed methodology yields insight into the origin of corrosion properties registered during standard electrochemical tests that are used to evaluate biomaterials.

1. Introduction

Commercially used Ti-based biomaterials have demonstrated a high corrosion resistance in many standard laboratory tests, including those performed according to the accepted ASTM protocol [1]. However, the degradation of these materials in the human body has been confirmed in clinical studies [2–5]. One of the major factors contributing the lower corrosion resistance *in vivo* is the production of aggressive species during periods of acute inflammation, which is a natural and necessary part of body's response to the harsh operative procedure [6]. Inflammatory-induced corrosion in artificial biological fluids has been simulated by the addition of reactive oxygen species (ROS), such as hydrogen peroxide (H_2O_2), that are produced by immune cells during their interaction with implant's surface [7–10]. Up to the present time, the effect of inflammatory species on the corrosion phenomena was studied mainly for widely-used Ti-based biomaterials such as commercially pure Ti (CP-Ti) [11–13] or Ti-6Al-4V [7,14–16]. Accelerated corrosion in simulated inflammatory conditions was confirmed by electrochemical tests such electrochemical impedance spectroscopy (EIS). It was found that the enrichment of simulated body fluid in the H_2O_2 resulted in a significant drop of the oxide layer resistance value, designated from EIS tests [13,17,18].

Interaction between the immune system and a metallic biomaterial's surface can be described as a positive feedback loop, where inflammatory reactions induce corrosion and the corrosion induces further inflammation and so on. For these reasons, it is important to block the initial inflammatory-induced degradation of Ti-based biomaterials to avoid a cascade of undesirable reactions that can accelerate the corrosion process. This can be done by tailoring the chemical composition of titanium-based materials [19]. It was found that one of the vanadium-free titanium biomedical alloy, Ti-29Nb-13Ta-4.6Zr (TNTZ) is less prone to H_2O_2-induced corrosion compared to the CP-Ti [20,21]. TNTZ surface shows unique stability in the inflammatory conditions which was indicated by the low difference between the oxide layer resistance values designated in the phosphate-buffered saline (PBS) and PBS + H_2O_2. Current conclusions related to TNTZ behavior during inflammation are based on the *in situ* electrochemical and immersion tests that are followed by post-immersion X-ray photoelectron spectroscopy (XPS) or

* Corresponding author at: NOMATEN Centre of Excellence, National Centre for Nuclear Research, A. Sołtana 7, 05-400 Otwock-Swierk, Poland.
E-mail address: agata.sotniczuk@ncbj.gov.pl (A. Sotniczuk).

https://doi.org/10.1016/j.apsusc.2024.160309
Received 26 February 2024; Received in revised form 13 May 2024; Accepted 16 May 2024
Available online 18 May 2024

focused ion beam combined with transmission electron microscopy (FIB-TEM) studies [19]. However, this approach does not give information related to the kinetics of the processes that contribute to the corrosion of implantable devices, precisely (i) oxide layer growth, and (ii) dissolution. Moreover, removing materials from the tested fluid and characterizing them by microscopy techniques, which requires using high vacuum, undoubtedly changes the hydrated oxide that is formed in the inflammatory environment [22].

These drawbacks can be overcome by exploiting atomic emission spectroelectrochemistry (AESEC) and *in situ* AFM techniques. AESEC monitors the dissolution of the alloying elements during exposure of the tested materials to a fluid *in situ* and in the real-time. In turn, *in situ* AFM gives an opportunity to observe oxide layer changes *in situ* and in the real-time during immersion and provides near atomic level information about the surface evolution in the liquid [22,23]. Both *in situ* AFM and AESEC methods are unexploited in the case of widely investigated vanadium-free titanium biomedical alloys, such as TNTZ [24]. Combining this two techniques gives a possibility to verify if the superior initial oxide layer resistance observed for titanium alloy [20] is related only to the suppressed dissolution or whether less pronounced oxide layer formation also contribute to this phenomenon. Hence, in this study we monitored the initial real-time inflammatory-induced corrosion process of CP-Ti and TNTZ alloy by both *in situ* AFM and AESEC techniques. Moreover, we provided the first evidence of how altering surface features of vanadium-free titanium alloy by its chemical etching influences the mechanism of inflammatory-induced corrosion. Proposed research methodology opens a new avenue for the *in vitro* safety verification of currently under development titanium biomaterials and their surface modification or functionalization.

2. Materials and methods

2.1. Materials and solution preparation

CP-Ti and Ti-29Nb-13Ta-4.6Zr (TNTZ) in the recrystallized states were used in this study. Grain sizes designated for tested materials were as follows: (i) CP-Ti: 46 ± 16 μm, (ii) TNTZ: 113 ± 44 μm (Fig. 1) Details about fabrication of the tested materials are provided elsewhere [19,20]. Before corrosion tests, samples were ground using SiC abrasive paper with following gradation: #600, #1200, and #2400. The grinding process was followed by polishing with a mixture of colloidal silica suspension with 0.04 μm particle size (OP-S, Struers) and H_2O_2 (30 wt% in water, Sigma Aldrich). Part of the samples were then subjected to the chemical etching using Kroll's reagent with following composition: 2 % HF + 4 % HNO_3 + H_2O. The aim of this procedure was to reveal grain boundaries and to increase nanotopography within the grains. Surface preparation procedures were performed three days before each test. Immediately before measurements, samples were re-polished for one minute and cleaned in isopropanol.

Inflammatory-induced degradation was tested in PBS + H_2O_2 solution which was prepared by dissolving PBS tablet (Sigma Aldrich) in deionized water. Inflammatory fluid *in vivo* contains variety of ROS such as H_2O_2, HOCl or radicals. However, standard biological fluids (such as PBS) enriched with H_2O_2 are commonly accepted to study inflammatory-induced corrosion as H_2O_2 can act itself as an intermediate compound of reactions that are taking place on biomaterial surface which simulates complex post-operative environment [9–11,25]. Physiological concentration of H_2O_2 that was measured in extracellular environments is reported to be in the μM range [18]. However, it has to be mentioned that locally, H_2O_2 content can reach the mM level (especially within the crevices when the exchanging of the solution is limited) and can, in fact, be generated by reduction reactions at metal electrode surfaces [26]. *In vitro* experiments exploited mostly supraphysiological concentration of H_2O_2 (from 33 mM [18] to 100 mM [7,14]). This approach accelerates corrosion processes leading to a decrease in experimental time necessary to observe possible H_2O_2-induced degradation [25]. This is important especially for the real-time *in situ* techniques, which requires constant monitoring of experiments. In this study, we decided to use the lowest concentration of H_2O_2 from those mentioned above (33 mM = 0.1 % H_2O_2) which is the closest to the realistic conditions and simultaneously gave us a chance to visualize surface changes in reasonable time and to detect titanium dissolution.

2.2. Real-time analysis of the surface evolution in the inflammatory fluid: in situ AFM

Surface topography analysis included following steps: (i) AFM scanning in air in order to set the distance between the tip and sample surface, (ii) the addition of an approximate 500 μl droplet of the PBS + 0.1 % H_2O_2 on the sample surface, and (iii) re-engaging the tip in the solution and performing AFM scanning in the solution. AFM measurements were conducted in the direct contact mode using Dimension ICON AFM, Bruker and ScanAsyst Fluid probe. Data visualization and numerical analysis were performed with the NanoScope Analysis, Bruker software.

2.3. Real-time dissolution monitoring in the inflammatory fluid: AESEC

Ion-dissolution monitoring was performed with a flow cell that was combined with an inductively coupled plasma atomic emission

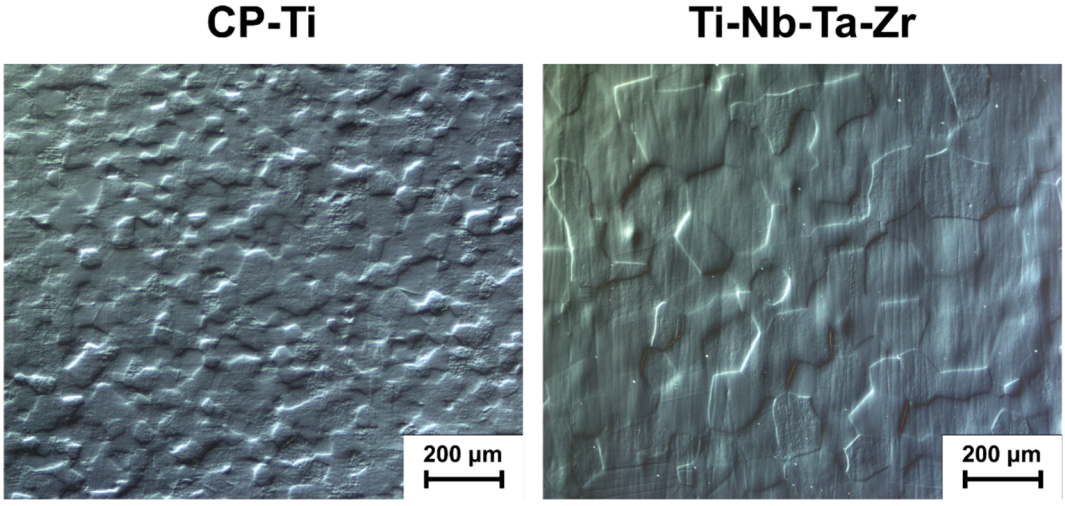

Fig. 1. Microstructure of tested materials visualized using light microscope.

spectrometer (ICP-AES), a Horiba Ultima 2C coupled with a three-electrode electrochemical flow cell with a saturated calomel reference electrode and Pt wire counter electrode. The reference and counter electrodes were separated from the sample by a porous membrane. The flow rate of the tested fluid (PBS + 0.1 % H_2O_2) was 1 ml per minute. Ti emission was measured at the wavelength 337.279 nm. All of the tests were calibrated by conventional methods of ICP-AES analysis using normalized standards. Detection limit for particular elements were as follows: (i) CP-Ti: Ti = 1.9 ppb, (ii) TNTZ: Ti: 1.9 ppb, Nb: 8.3 ppb, Ta: 15.7 ppb, Zr: 3.4 ppb. The elemental dissolution rate (ν_M) was designated according to the mathematical formulas that are presented elsewhere [27]. Electrode potential was monitored with a Gamry Reference 600, Potentiostat/galvanostat.

3. Results

The evolution of the oxide layer morphology was studied by *in situ* AFM observations conducted for 90 min in the droplet of PBS + H_2O_2 (Fig. 2). For CP-Ti, two groups of the oxide domes could be distinguished: (i) larger oxide domes with few nm in height and c.a. 0.5–1 μm lateral dimension, (ii) smaller oxide domes with a less than 1 nm in height and less than 0.5 μm lateral dimension (Fig. 2). It can be noticed that the larger domes remain almost stable in size during 90 min of immersion. The smaller oxide domes, however, tend to coalescence during immersion, which results in a flattening of the surface. Firstly, oxide domes were formed at the preferred sites of the surface that are characterized by enhanced reactivity (e.g. grain boundaries, impurities, interstitials) and subsequently grew in height up to a critical level. Then, in the surrounding planar regions, smaller domes are created, which resulted in a complete surface coverage after 30 min in PBS + H_2O_2 (Fig. 2). Conversely, no morphological changes in the surface layer were observed for TNTZ during immersion in the PBS + H_2O_2. Based on the topography profiles it can be assumed that the oxide layer formed on TNTZ alloy was stable during the whole immersion period (Fig. 2). This

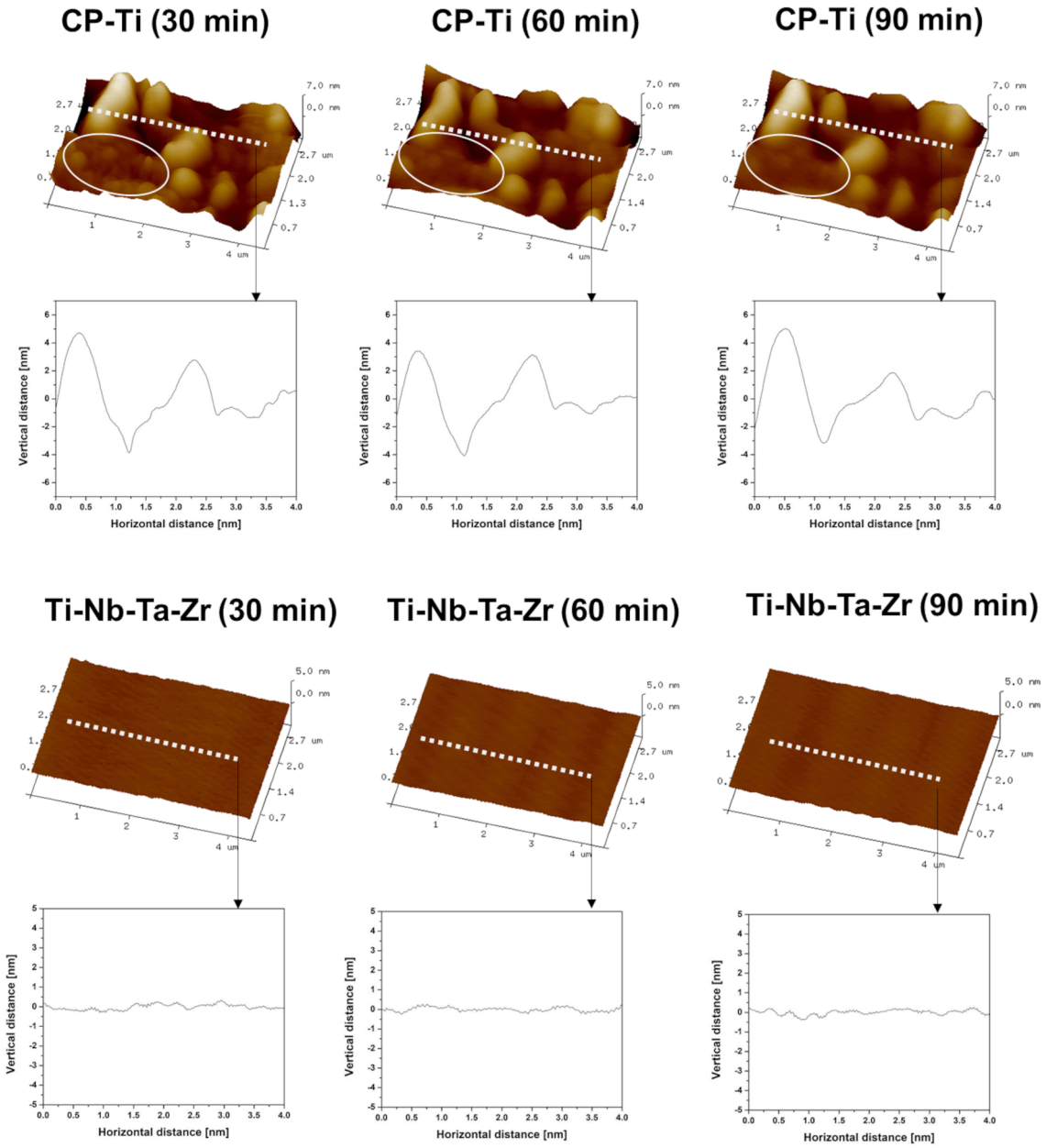

Fig. 2. Monitoring of the oxide layer changes during immersion of polished CP-Ti and TNTZ in PBS + H_2O_2: *in situ* AFM study. Note the smoothing of the surface oxides over time for CP-Ti and the smooth and non-varying nature of TNTZ surfaces.

indicates that the lattice diffusion of oxygen vacancies and titanium interstitials, which determine the solution growth of titanium oxide layers, is hindered in case of TNTZ alloy.

The differences between the oxide formation processes of CP-Ti and TNTZ in the polished state, may be attributed to the differential chemical compositions of the oxides formed on their surfaces. However, the surfaces of real implantable materials are usually functionalized e.g. by altering their topography in order to stimulate desired biological responses during osseointegration process [28]. A change in surface topography can affect the oxide layer stability during immersion in the fluid, which may affect the kinetics of oxide dome nucleation and growth. To study this phenomenon, *in situ* AFM experiments were repeated for the samples subjected to chemical etching in the mixture of HF and HNO_3 acids (Kroll agent). Fig. 3 illustrates the surface morphology in the vicinity of selected triple point revealed for CP-Ti and TNTZ respectively. AFM micrographs captured in air confirmed that that surface etching in the Kroll agent developed nanoscale roughness within the grain interiors. In case of TNTZ, the etched surface is significantly smoother, which is reflected by a visibly lower value of the arithmetic roughness (R_a) compared to CP-Ti (Fig. 4).

In addition to the presence of lower surface roughness within the grains, the relative difference between the height of grain boundaries and grain interiors is also significantly lower for TNTZ (Fig. 3). It can be noticed that for CP-Ti, the vertical distance between the lowest and the highest point did not change significantly after its immersion in the fluid (165 nm – distance in air, and 167 nm – distance after 90 min of immersion). This indicates that the kinetics of oxide layer growth in PBS + H_2O_2 (under steady-state conditions) is similar within both grain interiors and grain boundaries (Fig. 3). Contrary conclusions can be derived from the AFM observations performed for the etched TNTZ alloy (Fig. 3). It was found that immediately after immersion, the vertical distance between the highest and the lowest features is reduced for approximately 15 nm, which confirms that for TNTZ alloy oxide layer growth is more pronounced within the area of grain boundaries. For both CP-Ti and TNTZ, rapid nucleation of the oxide domes was observed after their immersion in PBS + H_2O_2 (Fig. 4).

In addition to oxide growth, a major contribution to corrosion is the dissolution of the alloy. The dissolution of Ti was measured directly during immersion in PBS + H_2O_2 using AESEC. Typical dissolution profiles are shown in Fig. 5. The electrolyte came into contact with the sample at $t = 0$ and the dissolution rates and open circuit potential were followed for 1200 s. For $t < 0$ was the background emission due to the electrolyte alone. At $t = 0$, a significant increase of detected Ti ions was visible as a dissolution peak around 0–50 s. After c.a. 200 s, the Ti

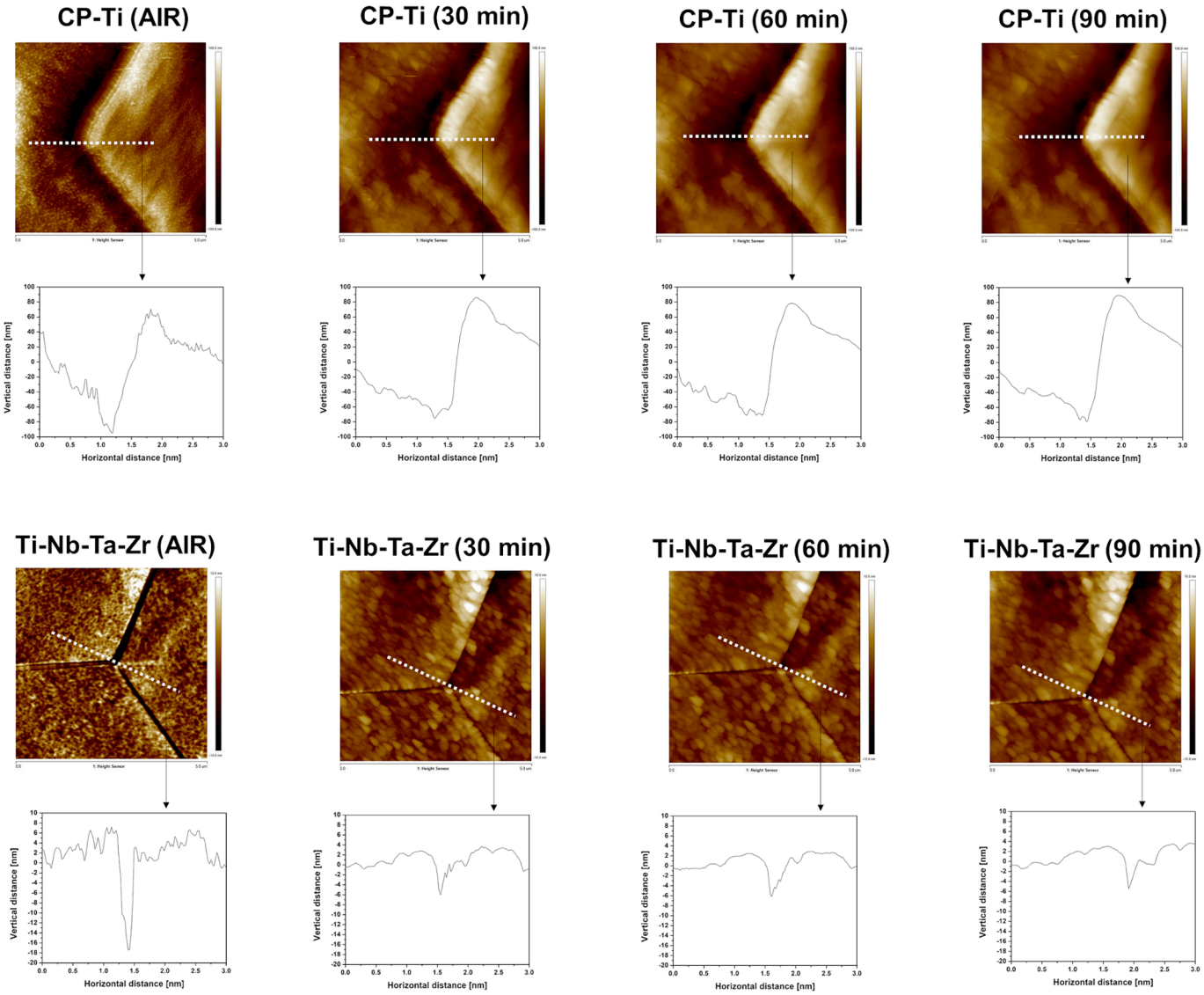

Fig. 3. Monitoring of the oxide layer changes during immersion of etched CP-Ti and TNTZ in PBS + H_2O_2: *in situ* AFM study.

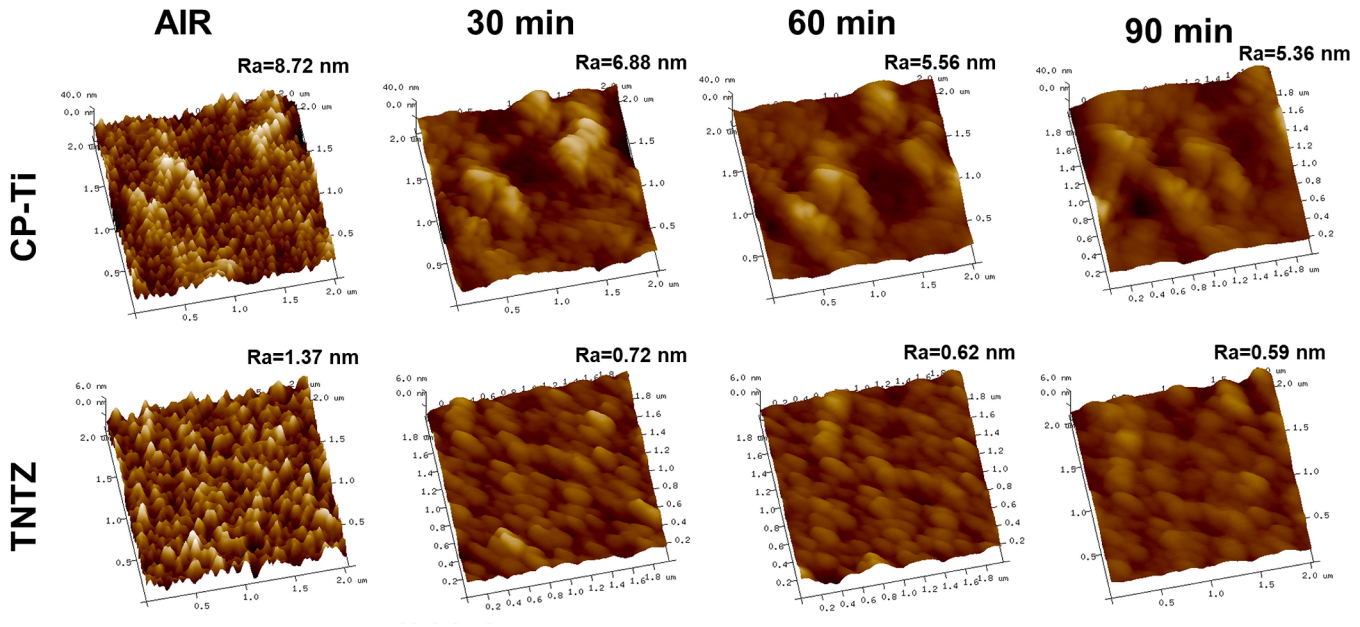

Fig. 4. Monitoring of the oxide layer changes within the grain interior of CP-Ti and TNTZ during immersion of etched samples in PBS + H_2O_2: *in situ* AFM study.

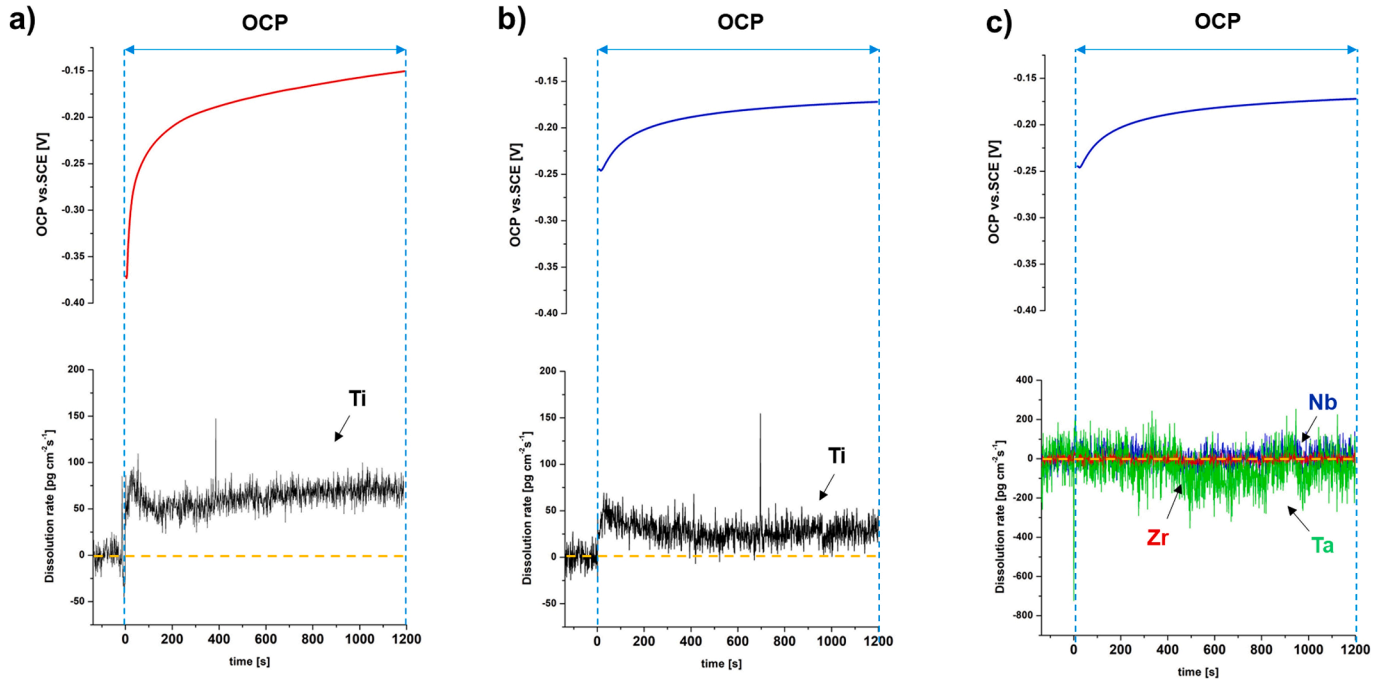

Fig. 5. Real-time monitoring of chemical elements dissolution during immersion of (a) CP-Ti and (b), (c) TNTZ in the flowing PBS + H_2O_2 solution.

dissolution rate stabilized for both materials. For both CP-Ti and TNTZ, the Ti signal was detectable during the whole time of AESEC analysis at the steady-state conditions (Fig. 5). In order to compare the amount of Ti ions dissolved into the fluid from tested materials, the average value of the dissolution rate was calculated based the data between 200 s and 1200 s. Single high peaks detected for CP-Ti c.a. at 400 s and for TNTZ c. a. 700 s were not included in the calculations (Fig. 5). Average dissolution rate of CP-Ti was calculated as 64 pg * cm^{-2} * s^{-1}, while for TNTZ alloy the value was found to be c.a. 2.4 times lower (27 pg * cm^{-2} * s^{-1}). Note that considering stoichiometry of TNTZ (Ti content 53.4 wt%) AESEC results revealed that dissolution of Ti in TNTZ was suppressed compared to CP-Ti. Contrary to Ti, the dissolution of alloying elements in TNTZ alloy (Nb, Ta, and Zr) was below the detection limit. Apart from the higher dissolution rate, the more substantial change in OCP value was observed for CP-Ti (Fig. 5).

4. Disscusion

By combining *in situ* AFM and AESEC analysis, oxide film formation and dissolution phenomena could be distinguished during the corrosion of the standard CP-Ti and the relatively novel vanadium-free titanium alloy (TNTZ). Consequently, the proposed methodology provides an opportunity to understand the origin of differences between CP-Ti and TNTZ corrosion behavior that were found based on the standard electrochemical tests performed in the simulated inflammatory fluid. AFM experiments revealed that oxide layer formed on the CP-Ti surface is

rebuilt rapidly after its contact with PBS + H_2O_2, which is reflected in the nucleation of oxide domes. When the nanometric, air-formed oxide layer is exposed to the fluid, ions and electrons diffuse across the oxide which results in its evolution [29]. Transfer of Ti ions across the film introduces tensile stresses at the Ti/oxide boundary, which consequently results in the formation of the oxide domes as can be seen from the AFM micrographs captured after 30 min of immersion (Fig. 2). With the increase of immersion time adjacent oxide domes tend to coalescence which should suppress the ion transport across the oxide. This can be responsible for the significant enhancement of corrosion resistance which was observed for CP-Ti after a long term (24 h) immersion in the PBS + H_2O_2 [13]. However, despite surface smoothening, nucleation of the new oxide domes was observed after 90 min of CP-Ti immersion (Fig. 2). The constant formation of the oxide domes in simulated inflammatory body fluid explain the increase of titanium oxide layer thickness up to several dozens of nm after a few years of exposure to the human body conditions [30]. Nucleation and further coalescence of the oxide domes in PBS + H_2O_2 is in agreement with previous research performed for CP-Ti tested in the standard PBS solution [22].

Contrary to CP-Ti, no inflammatory-induced morphological changes were detected for polished TNTZ during its 90 min of exposure to the PBS + H_2O_2 (Fig. 2). Both tested materials were mirror-like polished and demonstrated the same type of recrystallized structure, which consist of defect-free micrometric grains [13,19]. For this reason, it can be assumed that suppressed oxide growth for TNTZ alloy is strictly related to the complex chemical composition of the native oxide layer formed on its surface. Indeed, previous post-immersion XPS studies revealed that unique behavior of TNTZ can be related to the presence of Zr in the bulk alloy and thereby ZrO_2 on its surface [19]. It was found that the transformation from Zr to ZrO_2 is preferential during long-term of TNTZ exposure to the PBS + H_2O_2 solution [19]. This can be related to the slightly lower oxide formation energy for ZrO_2 (−1100.6 kJ/mol) [31] compared to the TiO_2 (−992 kJ/mol) [32] Results obtained for binary Ti-Zr alloy indicate that contrary to Ti and TiO_2, Zr and ZrO_2 are not prone to form the complex compounds with H_2O_2 [15]. Unique stability of ZrO_2 in the biological fluid can be associated with higher dissociation energy for Zr-O bonds (766 kJ/mol) than for Ti-O bonds (666 kJ/mol) [33]. High strength of Zr-O bonds can prevents ZrO_2 disruption in H_2O_2-rich solution. Findings related to the beneficial role of Zr on the suppression of H_2O_2-induced degradation were confirmed by gradually decreasing susceptibility to corrosion with the increasing content of Zr in binary Ti-Zr alloys. It was found that increasing of Zr concentration in Ti-Zr alloys resulted in the reduction of OCP value which can be related to suppression of cathodic reactions [15]. Finally, it has to be mentioned that ZrO_2 act as a catalyzer for H_2O_2 decomposition [34]. This can possibly result in a rapid decrease of H_2O_2 content in PBS surrounded TNTZ alloy, making testing fluid less aggressive. Consequently, the presence of ZrO_2 in TNTZ oxide layer could partially block the H_2O_2-induced transformation of TiO_2 oxide, which could be the reason for the lack of morphological changes observed for TNTZ during short, 90 min *in situ* AFM observations. It can be concluded that short-term *in situ* AFM experiments performed for the mirror-like TNTZ surface, did not allow to observe any morphological changes that can help to understand the process of the inflammatory-induced evolution of the oxide film. Gaining this knowledge was possible by performing *in situ* AFM tests for the chemically treated materials. These experiments revealed that TNTZ oxide film growth follows a similar mechanism as was observed for CP-Ti, which involves the nucleation of the oxide domes and their further coalescence, ultimately leading to surface smoothening (Fig. 4).

Apart from suppressed H_2O_2-induced oxide growth, TNTZ alloy also demonstrated a lower tendency to dissolution in the inflammatory fluid compared to the standard CP-Ti. AESEC measurements revealed that the dissolution rate of elemental Ti was c.a. 2.4 times lower for TNTZ alloy. It should be kept in mind that a mass content of Ti in tested TNTZ material exceeded 50 %, which indicates that dissolution rate of this element should not be lower than 2 times compared to the CP-Ti. Moreover, the dissolution of the alloying elements in TNTZ (Nb, Ta, and Zr) was under their respective detection limit. However, considering the overall results of both *in situ* AFM and AESEC analysis, it can be concluded that the initial, inflammatory-induced corrosion process of TNTZ alloy is associated rather with the dissolution of Ti. Oxide layer growth does not participate directly in the corrosion phenomena in the simulated inflammatory fluid.

5. Conclusions

This work presents a new approach to biomaterials testing that permits *in situ* monitoring of both dissolution and oxide layer growth phenomena that contribute to the overall corrosion process. Application of this methodology offers insight into the origin of corrosion behavior detected during standard electrochemical tests, such as EIS, that are commonly used for evaluating functional properties of newly designed biomaterials. Moreover, this study provides the first evidence that at the steady-state conditions, as can be found in the human body, noticeable dissolution occur for both CP-Ti and TNTZ alloy immediately after their immersion in simulated inflammatory fluid (PBS + H_2O_2). Combining *in situ* AFM and AESEC results demonstrates that the H_2O_2-induced corrosion processes involve both dissolution and oxide growth for CP-Ti, while dissolution is the major contribution for the TNTZ alloy. Oxide film growth process of TNTZ is suppressed by the complex composition of the oxide layer that is spontaneously air-formed on its surface, at least for the material in the mirror-like polished state. Roughening of TNTZ surface by its chemical etching led to a rapid oxide layer growth in the PBS + H_2O_2, which was reflected by complete surface coverage with the oxide domes. *In situ* AFM experiments for the chemically activated materials indicate that the H_2O_2-induced growth of the oxide for TNTZ alloy follow the same mechanism as was found for CP-Ti.

CRediT authorship contribution statement

Agata Sotniczuk: Writing – original draft, Project administration, Methodology, Investigation, Funding acquisition, Conceptualization. **Baojie Dou:** Writing – review & editing, Methodology, Investigation. **Yangping Liu:** Writing – review & editing, Methodology, Investigation. **Oumaïma Gharbi:** Methodology, Writing – review & editing. **Fan Sun:** Writing – review & editing, Resources. **Halina Garbacz:** Funding acquisition, Writing – review & editing. **Jeremy L. Gilbert:** Writing – review & editing, Supervision, Resources, Conceptualization. **Kevin Ogle:** Writing – review & editing, Supervision, Resources, Conceptualization.

Declaration of competing interest

The authors declare that they have no known competing financial interests or personal relationships that could have appeared to influence the work reported in this paper.

Data availability

The raw/processed data required to reproduce these findings cannot be shared at this time as the data also forms part of an ongoing study.

Acknowledgments

AFM research were financially supported by the Polish National Agency for Academic Exchange (NAWA) under the Iwanowska program [grant agreement: PPN/IWA/2019/1/00084/U/00001]. AESEC research were financially supported by the Excellence Initiative Research University, Warsaw University within the Mobility PW program [grant agreement: 1820/107/Z09/2023]. During writing manuscript AS was partially funded through the European Union Horizon 2020 research and innovation program under Grant Agreement No.

857470 and from the European Regional Development Fund under the program of the Foundation for Polish Science International Research Agenda PLUS, grant No. MAB PLUS/2018/8, and the initiative of the Ministry of Science and Higher Education 'Support for the activities of Centers of Excellence established in Poland under the Horizon 2020 program' under agreement No. MEiN/2023/DIR/3795."

References

[1] F. Yu, O. Addison, A.J. Davenport, A synergistic effect of albumin and H2O2 accelerates corrosion of Ti6Al4V, Acta Biomater. 26 (2015) 355–365, https://doi.org/10.1016/j.actbio.2015.07.046.
[2] J.L. Gilbert, S. Mali, R.M. Urban, C.D. Silverton, J.J. Jacobs, In vivo oxide-induced stress corrosion cracking of Ti-6Al-4V in a neck–stem modular taper: Emergent behavior in a new mechanism of in vivo corrosion, J. Biomed. Mater. Res. Part B Appl. Biomater. 100 (2012) 584–594.
[3] P. Jiang, Y. Zhang, R. Hu, B. Shi, L. Zhang, Q. Huang, Y. Yang, P. Tang, C. Lin, Advanced surface engineering of titanium materials for biomedical applications: from static modification to dynamic responsive regulation, Bioact. Mater. 27 (2023) 15–57.
[4] D.J. Hall, R. Pourzal, J.J. Jacobs, R.M. Urban, Metal wear particles in hematopoietic marrow of the axial skeleton in patients with prior revision for mechanical failure of a hip or knee arthroplasty, J. Biomed. Mater. Res. Part B Appl. Biomater. 107 (2019) 1930–1936.
[5] B.E. Nagay, J.M. Cordeiro, V.A.R. Barao, Insight into corrosion of dental implants: from biochemical mechanisms to designing corrosion-resistant materials, Curr. Oral Heal. Reports. 9 (2022) 7–21.
[6] J.L. Gilbert, G.W. Kubacki, Oxidative stress, inflammation, and the corrosion of metallic biomaterials: corrosion causes biology and biology causes corrosion, in: Oxidative Stress Biomater, Elsevier, 2016, pp. 59–88.
[7] M. Prestat, F. Vucko, L. Holzer, D. Thierry, Microstructural aspects of Ti6Al4V degradation in H2O2-containing phosphate buffered saline, Corros. Sci. (2021).
[8] J.L. Gilbert, S. Sivan, Y. Liu, S.B. Kocagöz, C.M. Arnholt, S.M. Kurtz, Direct in vivo inflammatory cell-induced corrosion of CoCrMo alloy orthopedic implant surfaces, J. Biomed. Mater. Res. Part A. 103 (2015) 211–223.
[9] C. Fonseca, M. Barbosa, Corrosion behaviour of titanium in biofluids containing H2O2 studied by electrochemical impedance spectroscopy, Corros. Sci. 43 (2001) 547–559, https://doi.org/10.1016/S0010-938X(00)00107-4.
[10] J. Pan, D. Thierry, C. Leygraf, Hydrogen peroxide toward enhanced oxide growth on titanium in PBS solution: blue coloration and clinical relevance, J. Biomed. Mater. Res. Off. J. Soc. Biomater. Japanese Soc. Biomater. 30 (1996) 393–402.
[11] G. Mabilleau, S. Bourdon, M.L. Joly-Guillou, R. Filmon, M.F. Baslé, D. Chappard, Influence of fluoride, hydrogen peroxide and lactic acid on the corrosion resistance of commercially pure titanium, Acta Biomater. 2 (2006) 121–129, https://doi.org/10.1016/j.actbio.2005.09.004.
[12] A. Fonseca-García, J. Pérez-Alvarez, C.C. Barrera, J.C. Medina, A. Almaguer-Flores, R.B. Sánchez, S.E. Rodil, The effect of simulated inflammatory conditions on the surface properties of titanium and stainless steel and their importance as biomaterials, Mater. Sci. Eng. C. 66 (2016) 119–129, https://doi.org/10.1016/j.msec.2016.04.035.
[13] A. Sotniczuk, W. Chromiński, B. Adamczyk-Cieślak, M. Pisarek, H. Garbacz, Corrosion behaviour of biomedical Ti under simulated inflammation: exploring the relevance of grain refinement and crystallographic texture, Corros. Sci. 200 (2022) 110238.
[14] M.A. Kurtz, P. Khullar, J.L. Gilbert, Cathodic activation and inflammatory species are critical to simulating in vivo Ti-6Al-4V selective dissolution, Acta Biomater. 149 (2022) 399–409.
[15] Y. Zhang, A.J. Davenport, B. Burke, N. Vyas, O. Addison, Effect of Zr addition on the corrosion of Ti in acidic and reactive oxygen species (ROS)-containing environments, ACS Biomater. Sci. Eng. 4 (2018) 1103–1111.
[16] Y.S. Hedberg, F. Gamna, G. Padoan, S. Ferraris, M. Cazzola, G. Herting, M. Atapour, S. Spriano, I.O. Wallinder, Surface modified Ti6Al4V for enhanced bone bonding ability–effects of silver and corrosivity at simulated physiological conditions from a corrosion and metal release perspective, Corros. Sci. 168 (2020) 108566.
[17] E. Brooks, M. Tobias, K. Krautsak, M. Ehrensberger, The influence of cathodic polarization and simulated inflammation on titanium electrochemistry, J. Biomed. Mater. Res. - Part B Appl. Biomater. 102 (2014) 1445–1453, https://doi.org/10.1002/jbm.b.33123.
[18] Y. Zhang, O. Addison, F. Yu, B.C.R. Troconis, J.R. Scully, A.J. Davenport, Time-dependent enhanced corrosion of Ti6Al4V in the presence of H 2 O 2 and albumin, Sci. Rep. 8 (2018) 3185.
[19] A. Sotniczuk, J.L. Gilbert, Y. Liu, M. Matczuk, W. Chromiński, D. Kalita, M. Pisarek, H. Garbacz, Corrosion resistance of β-phase titanium alloys under simulated inflammatory conditions: exploring the relevance of biocompatible alloying elements, Corros. Sci. 220 (2023) 111271.
[20] A. Sotniczuk, D. Kuczynska-Zemla, P. Kwasniak, M. Thomas, H. Garbacz, Corrosion behavior of Ti-29Nb-13Ta-4.6Zr and commercially pure Ti under simulated inflammatory conditions - comparative effect of grain refinement and non-toxic beta phase stabilizers, Electrochim. Acta. (2019), https://doi.org/10.1016/J.ELECTACTA.2019.04.138.
[21] M. Prestat, D. Thierry, Corrosion of titanium under simulated inflammation conditions: clinical context and in vitro investigations, Acta Biomater. 136 (2021) 72–87.
[22] J.P. Bearinger, C.A. Orme, J.L. Gilbert, Direct observation of hydration of TiO2 on Ti using electrochemical AFM: freely corroding versus potentiostatically held, Surf. Sci. 491 (2001) 370–387.
[23] J.P. Bearinger, C.A. Orme, J.L. Gilbert, In situ imaging and impedance measurements of titanium surfaces using AFM and SPIS, Biomaterials. 24 (2003) 1837–1852.
[24] M. Niinomi, M. Nakai, J. Hieda, Development of new metallic alloys for biomedical applications, Acta Biomater. 8 (2012) 3888–3903, https://doi.org/10.1016/j.actbio.2012.06.037.
[25] M.A. Kurtz, K. Alaniz, L.M. Taylor, A. Moreno-Reyes, J.L. Gilbert, Increasing temperature accelerates Ti-6Al-4V oxide degradation and selective dissolution: an Arrhenius-based analysis, Acta Biomater. (2024).
[26] M.J. Wiegand, T.Z. Benton, J.L. Gilbert, A fluorescent approach for detecting and measuring reduction reaction byproducts near cathodically-biased metallic surfaces: reactive oxygen species production and quantification, Bioelectrochemistry. 129 (2019) 235–241.
[27] J. Han, A.Y. Gerard, P. Lu, J.E. Saal, K. Ogle, J.R. Scully, Elementally resolved dissolution kinetics of a Ni-Fe-Cr-Mn-Co multi-principal element alloy in sulfuric acid using AESEC-EIS, J. Electrochem. Soc. 169 (2022) 81507.
[28] L. Wang, W. Zhou, Z. Yu, S. Yu, L. Zhou, Y. Cao, M. Dargusch, G. Wang, An in vitro evaluation of the hierarchical micro/nanoporous structure of a Ti3Zr2Sn3Mo25Nb alloy after surface dealloying, ACS Appl. Mater. Interfaces. 13 (2021) 15017–15030.
[29] D.D. Macdonald, The point defect model for the passive state, J. Electrochem. Soc. 139 (1992) 3434.
[30] D.M. Brunette, P. Tengvall, M. Textor, P. Thomsen, Titanium in medicine: material science, surface science, engineering. Biological Responses and Medical Applications, Springer Science & Business Media, 2012.
[31] K.T. Jacob, Y. Waseda, Potentiometric determination of the gibbs energies of formation of SrZrO 3 and BaZrO 3, Metall. Mater. Trans. B. 26 (1995) 775–781.
[32] J.D. Cox, D.D. Wagman, V.A. Medvedev, CODATA key values for thermodynamics, 1989.
[33] Y.-R. Luo, J.A. Kerr, Bond dissociation energies, CRC Handb. Chem. Phys. 89 (2012) 65–98.
[34] C.M. Lousada, A.J. Johansson, T. Brinck, M. Jonsson, Mechanism of H2O2 decomposition on transition metal oxide surfaces, J. Phys. Chem. C. 116 (2012) 9533–9543.